Kovove Mater. 62 2024 223–234
DOI: 10.31577/km.2024.4.223

Study on microstructure and properties of typical copper foils

Jianhua Yang[1], Liping Wang[1], Zhongbo Bai[2], Xiaolin Peng[2], Baoxin Feng[2], Eryong Liu[1]*

[1]*School of Materials Science and Engineering, Xi'an University of Science and Technology, Xi'an 710054, P. R. China*
[2]*Lingbao Wason Copper Foil Co., Ltd, Henan 472500 Lingbao, P. R. China*

Received 18 Januar 2024, received in revised form 30 August 2024, accepted 6 September 2024

Abstract

With the rapid development of new energy vehicles, the requirements of high elongation and high conductivity are put forward for lithium battery copper foil. In this paper, the typical 6 μm lithium battery copper foil of four enterprises is taken as the research object, and the morphology, structure, and performance of lithium battery copper foil are studied. The results show that the surface condition of the cathode roll affects not only the brightness of the copper foil but also the mechanical properties of the copper foil. The copper foil with low residual stress can be obtained by controlling the grain size at a low level so that the proportion of the (220) crystal plane is much smaller than that of the (200) crystal plane. As the grain size of copper foil decreases, the tensile strength and elongation of copper foil gradually increase. The increase in the proportion of the (111) crystal plane increases the elongation, and the increase in the proportion of the (220) crystal plane increases the tensile strength. Thus, the basis for adjusting the performance of copper foil is determined, which lays a theoretical foundation for the subsequent study of the electrodeposition copper foil process.

K e y w o r d s: lithium battery copper foil, roughness, microstructure, crystal orientation, performance

1. Introduction

In the rapid development of today's electronic information industry, electrolytic copper foil is known as the 'neural network' of electronic product signal and power transmission and communication, which is widely used in the electronic industry [1, 2]. With the blowout growth of the new energy vehicle market, the power battery industry has ushered in rapid development while driving the shared prosperity of the upstream sector [3]. As the negative current collector of power batteries, electrolytic copper foil also has a sharp increase in demand with the vigorous development of the power battery industry [4]. Driven by the demand for power batteries to increase energy density and reduce the cost of kilowatt-hour, the iteration of copper foil thickness is accelerated [5], and the development of 'extremely thin' further enhances the technical and technological barriers of the electrolytic copper foil industry [7]. For example, 8 μm copper foil is widely used in LG, Samsung, and other enterprises [6], and some enterprises urgently need 6 μm or even 4.5 μm lithium battery copper foil. Therefore, the 'ultra-thinning' and the accompanying 'high strength and toughness' have driven the rapid development of lithium copper foil technology [8, 9].

The rapid development of the new energy automobile industry has put forward new requirements for lithium battery copper foil [10]. As the main development direction of domestic copper foil enterprises in the past two years, 6 μm lithium battery copper foil has problems of great technical difficulty, and only a few enterprises can meet the requirements of high-quality lithium battery copper foil [11, 12]. We urgently need to improve the production process of copper foil, determine the problems existing in the performance of copper foil, and establish a connection with the production process. This paper points out the direction for further optimizing the production process and improving the yield and quality of copper foil [13–15].

2. Experimental materials and methods

The experimental materials were 6 μm lithium

*Corresponding author: e-mail address: liueryong@xust.edu.cn

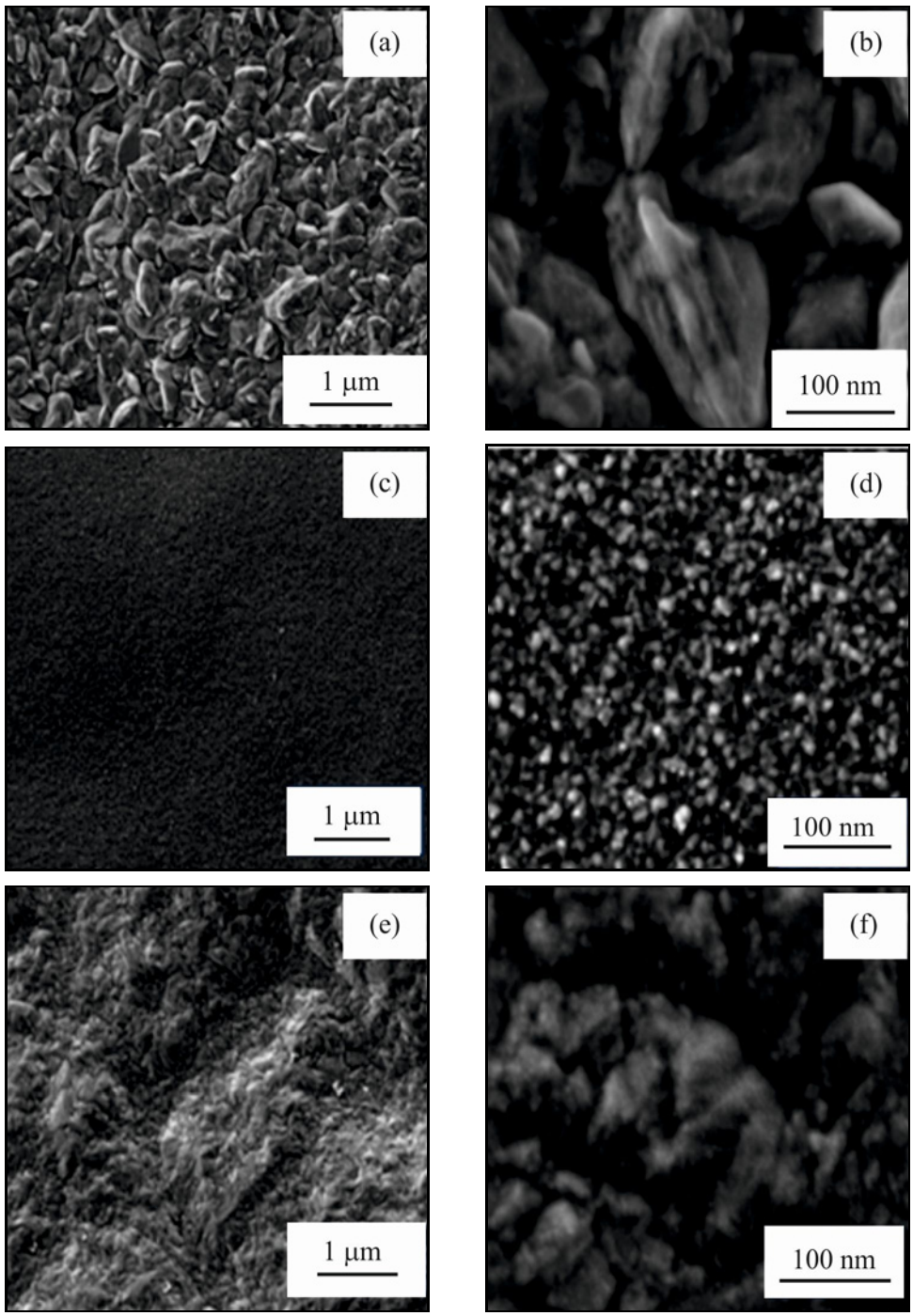

Fig. 1a–f. Microstructure of 6 μm copper foil from different enterprises: (a) CF-1 × 5000, (b) CF-1 × 50000, (c) CF-2 × 5000, (d) CF-2 × 50000, (e) CF-3 × 5000, (f) CF-3 × 50000.

battery copper foil produced by four manufacturers named CF-1, CF-2, CF-3, and CF-4. The rough surface, smooth surface, cross-section, and morphology of copper foil samples were characterized by a JSM--7900F field emission scanning electron microscope. Preparation steps of cross-section samples: The copper foil prepared by electrodeposition was sampled according to the size of 1 cm × 1 cm. After sampling, the inlaid sample was prepared into a cross-section sample, and then the inlaid cross-section sample was coarsely ground by a metallographic polishing machine. The sandpapers used in polishing were 280#, 500#, 800#, 1000#, 1500#, and 2000#, respectively. The surface of the sandpaper was kept wet during grinding, and the speed of the polishing machine was adjusted to about 600 r min^{-1}. After the rough grinding, the cross-section samples were polished with metallographic grinding paste; the parti-

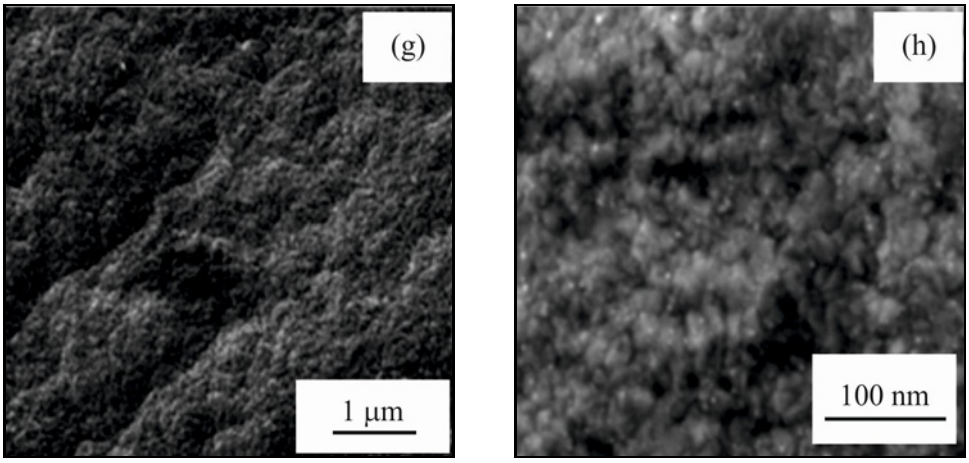

Fig. 1g,h. Microstructure of 6 μm copper foil from different enterprises: (g) CF-4 × 5000, and (h) CF-4 × 50000.

cle sizes were selected as W2.5, W1.5, and W0.5, respectively; during the polishing process, it is also necessary to maintain the wetting state of the surface of the polishing cloth and adjust the rotation speed of the polishing machine to about 600 r min^{-1}. After the sample is polished, it is corrupted. The hydrochloric acid solution with a volume fraction of 25 % FeCl3 was selected as the corrosion solution, and the corrosion time was 6–7 s. After the corrosion, the surface was washed with deionized water immediately, and the washing time was about 10 seconds until the corrosion solution on the surface was completely removed. After the washing, the sample's surface was dried immediately to prevent surface oxidation. The crystal orientation of copper foil samples was analyzed by SHIMAZDU XRD-7000 X-ray diffractometer. The copper foil samples prepared by electrodeposition were sampled according to the size of 1 cm × 1 cm, and the XRD phase analysis samples were prepared after the oxide layer on the surface of the copper foil was removed. The scanning range of the specimen was determined to be 30°–80° , and the scanning speed was 4° min^{-1}. After completing the test, MDI Jade 6.5 software analyzed and processed the experimental data. The grain size, crystal orientation, texture coefficient (TC), and residual stress of copper foil were analyzed. An SJ-301 roughness tester tested the surface roughness of copper foil. The sample was tiled to the horizontal plane, and the upper, middle, and lower positions were selected according to the length direction for testing. Each position was measured thrice, nine times, and the final result was the average value. To obtain different microstructures, copper foils from different manufacturers were placed in a high-temperature closed environment at 180 ℃ for 1 min. The same copper foil was cut into three samples of 12.7 mm × 152 mm × 6 μm by a special copper foil cutting machine. The tensile strength and elongation of copper foil were tested by the INSTRON3343-6997 copper foil tensile testing machine at room temperature.

3. Results and discussion

3.1. Micro-morphology of typical copper foil

3.1.1. Wool surface morphology

The microstructures of typical 6 μm electrolytic copper foils from different companies were obtained by scanning electron microscopy. The grain morphology, size, and distribution of the four copper foil samples differed significantly. The copper grains deposited on the rough surface of the CF-1 copper foil sample are relatively coarse, and the grain morphology is uniformly distributed on the surface in an irregular prismatic shape. The large grains are interlaced with fine grains. The grain size is between 1–2 μm (Fig. 1a). Due to the different grain sizes, there are apparent pores between the tightly arranged grains, and the densification of the copper foil is poor (Fig. 1b). The grain refinement of the copper foils deposited with CF-2 was found to be exceptionally high, which is much smaller than that of the grain sizes of the CF-1 deposited copper foils (Fig. 1c). The uniformity of the distribution of the copper grains is very high. The grain sizes are less than 100 nm. The refined copper grains indicate that during the electrodeposition process, the nucleation rate of copper grains is much higher than the growth rate. They can be uniformly deposited on the surface of the cathode rolls, which dramatically improves the densification of the copper foils and free the macroscopic and microscopic morphology of the foils from defects (Fig. 1d). From the macroscopic morphology of the sample of the CF-3 copper foils, it can be seen that there is an obvious undulation on the surface of the foils (Fig. 1e). The bond-

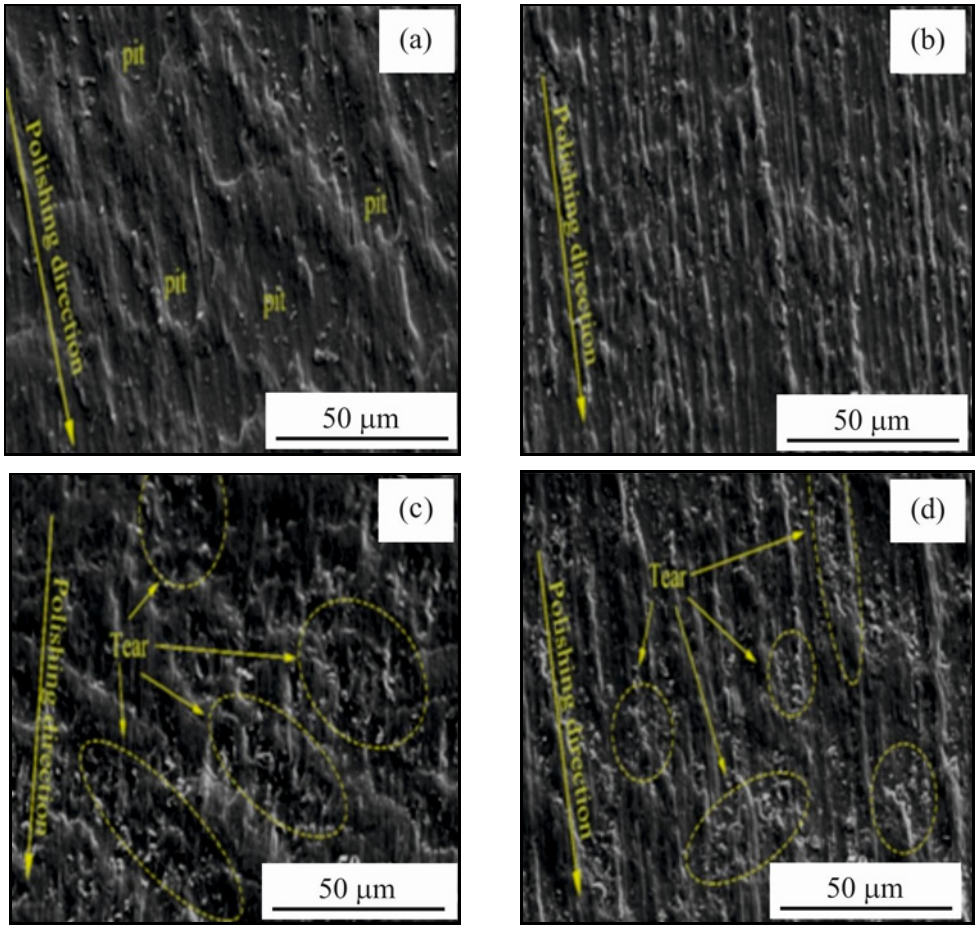

Fig. 2. Glossy micromorphology (× 1000) of 6 μm copper foil from different companies: (a) CF-1, (b) CF-2, (c) CF-3, and (d) CF-4.

ing between the clusters of copper grains is weaker, there are apparent pores, and the grain morphology is not good. There is a weak bonding between the copper grain clusters, apparent porosity, irregular grain morphology, and many refined grains with 100–300 nm scales in the depression, indicating that the grains of CF-3 copper foil are not uniformly distributed during the deposition process. There may be the phenomenon that the tips of the deposited grains preferentially nucleate by discharge while the undeposited areas nucleate slowly. In other words, the uneven current density distribution may lead to different grain growth rates, forming a fluctuating growth pattern (Fig. 1f). The morphology of the CF-4 Cu foil is similar to that of the CF-3 Cu foil (Figs. 1f,g). The surface is also undulating, but from the high-power morphology, it can be found that the undulation on the surface of the CF-4 Cu foil consists of refined grains with a grain size of about 100 nm. There are dark spots in individual positions in the figure, indicating that there are also high and low undulations between grains in the high-magnification mode. This reflects that although the CF-4 manufacturer can control the nucleation rate of copper grains during the deposition of copper foils, the current density cannot be uniformly distributed on the surface of the cathode roll.

3.1.2. Optical surface morphology

The smooth surface morphology of four typical six μm copper foils is shown in Fig. 2. The smooth surface of copper foils refers to the stripping surface of the titanium cathode roll, better reflecting the nucleation characteristics of copper foils. Since the smooth surface morphology of the copper foil is a replica of the cathode roll morphology, the surface quality of the cathode roll determines the smooth surface morphology of the copper foil.

The smooth surface of CF-1 copper foil is relatively rough, with many large pits along the polishing direction of the cathode roll, and minor copper grains are also distributed in the pits (Fig. 2a). The surface of CF-2 copper foil is a regular groove structure closely related to the polishing pattern of the titanium cathode roll (Fig. 2b). The surface of the CF-3 sample is not smooth, and the tearing of the copper foil leaves many craters and clusters of small copper grains. This indicates that the cathode rolls of CF-3 and CF-1 Cu

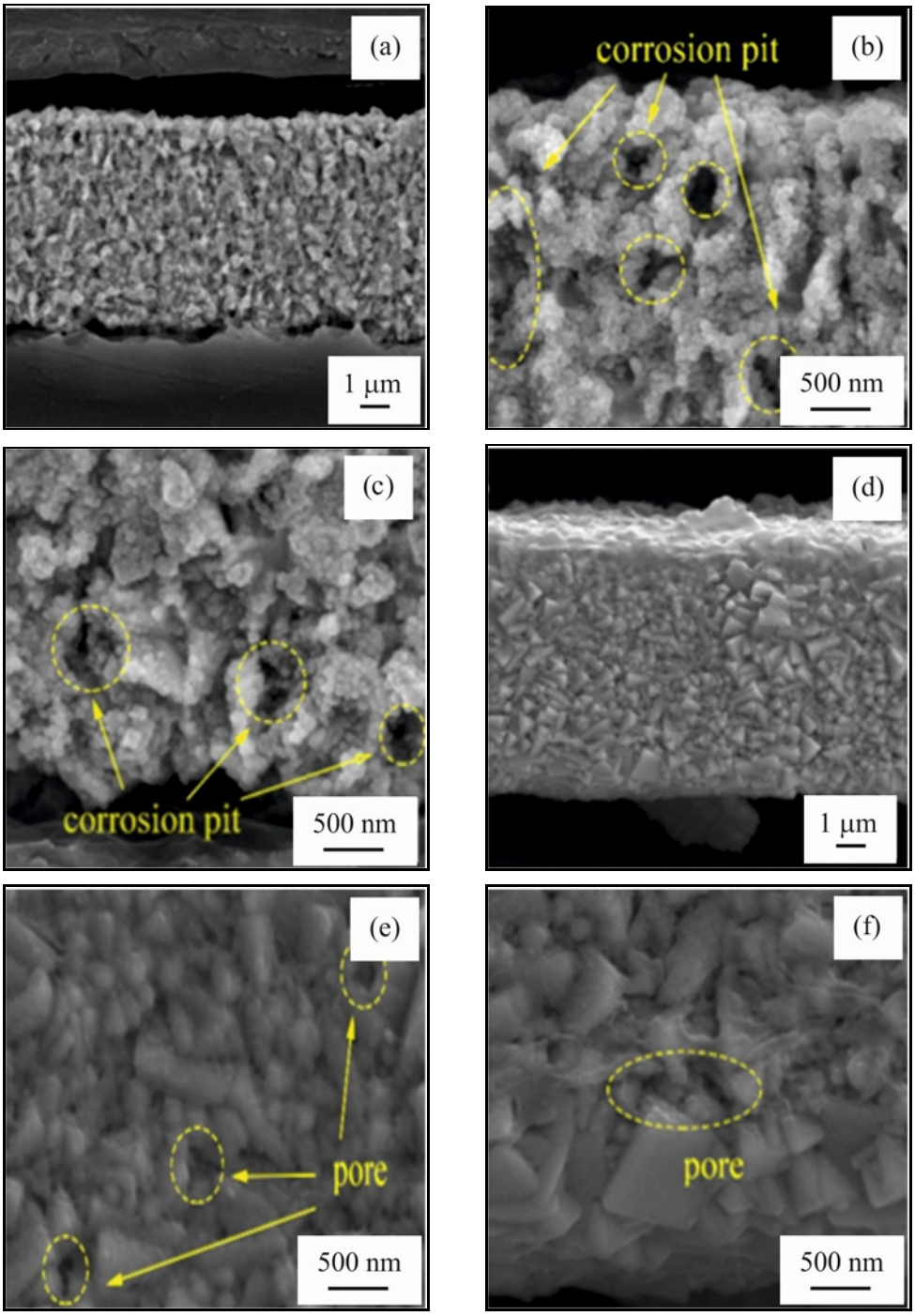

Fig. 3a–f. Microstructure of 6 μm copper foil sections of different enterprises: (a) CF-1 × 8000, (b) CF-1-S × 30000, (c) CF-1-M × 3000, (d) CF-2 × 8000, (e) CF-2-S × 30000, (f) CF-2-M × 30000.

foils were not well polished (Fig. 2c). The surface of the CF-4 sample was also uniformly distributed with traces of polished cathode rolls, which is similar to the characteristics of the CF-2 sample. However, the surface of CF-4 Cu foil still had small areas of craters after tearing, and some of the craters had more burrs (Fig. 2d). In general, the cratering characteristics of the surface of copper foil were closely related to the reason for the polishing treatment of the cathode rolls. For example, the presence of micro protrusions on the surface of the titanium cathode causes the deposited copper foil to be lifted by the small burrs of the roll and torn out of the craters of different sizes. It is imperative to reinforce the polishing control of the cathode roll to prevent alterations in the structure and properties of the copper foil, which may result from changes in the surface state of the cathode roll during the production process.

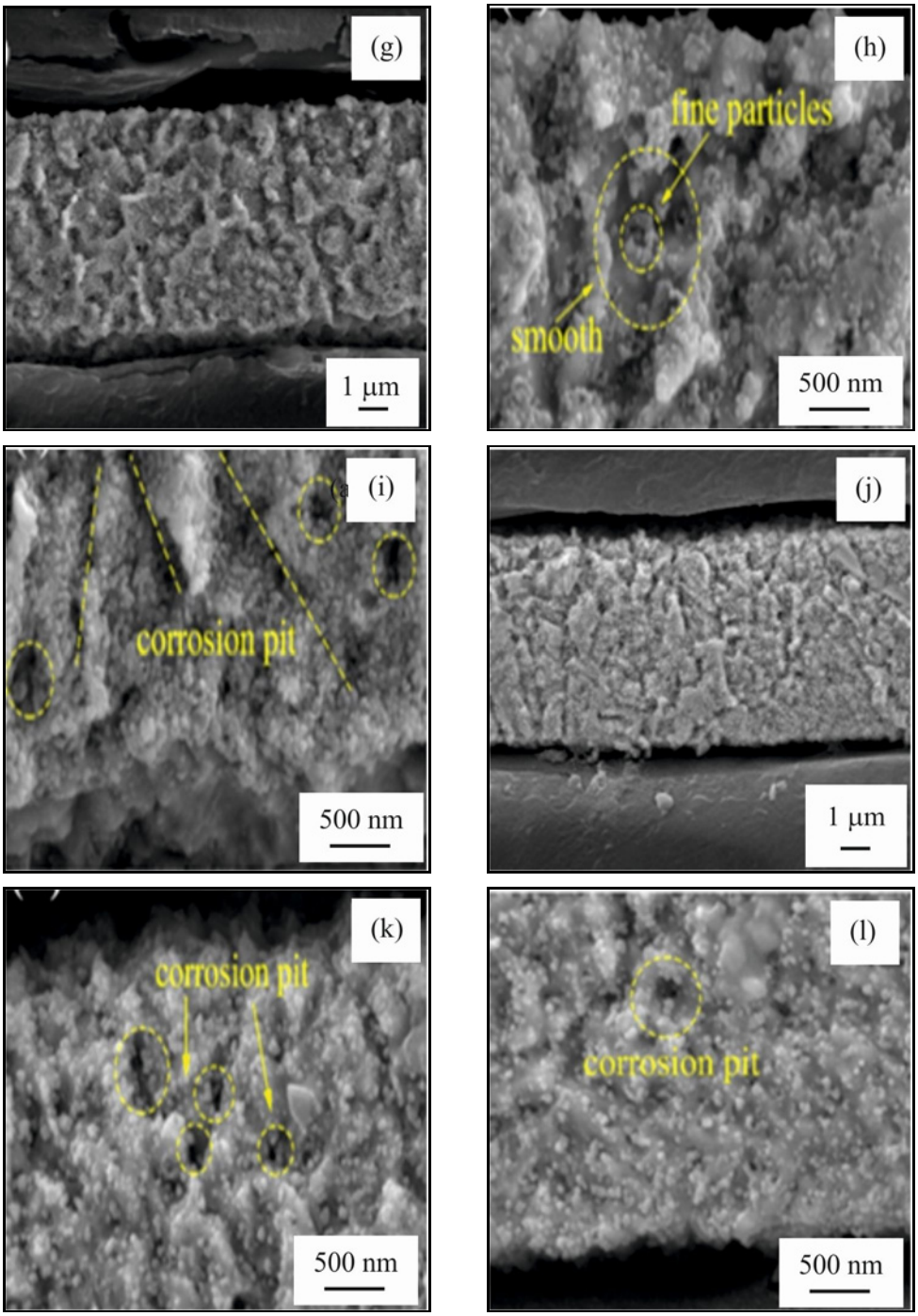

Fig. 3g–l. Microstructure of 6 μm copper foil sections of different enterprises: (g)CF-3 × 8000, (h) CF-3-S × 30000, (i) CF-3-M × 30000, (j) CF-4 × 8000, (k) CF-4-S × 30000, and (l) CF-4-M × 30000.

3.1.3. Cross-section morphology

The cross-section of a copper foil can reflect changes in the form of grain growth during electrodeposition. During electrodeposition, copper ions are reduced on the surface of the cathode roll, and copper grains accumulate layer by layer, forming copper foil. Thus, the growth process of copper foils goes through an initial epitaxial growth period, a transitional growth period, and finally, a growth period controlled by electrodeposition conditions. From the cross-section morphology, it can be seen that the corrosion resistance of the CF-1 samples is poor (Fig. 3a). The upper and lower parts of the cross-section are corroded by pits and fine particles of different depths, the bonding force between grains is weakened, and the mechanical strength is significantly reduced, which indicates that the grain boundaries between the grains of

copper foils have high energies, and are in an unstable state, which leads to the corrosion of the boundaries in the corrosive process is faster than that inside the grains.

The upper and lower parts of the CF-2 copper foil were not corroded with large corrosion pits and fine particles, and only the grains in the shallow area were corroded with individual small holes (Fig. 3b). This indicates that the bonding force between the grains of the copper foil is powerful, the grain boundaries have low energy, and the grain boundaries are stable, making it not easy to be corrupted by the grain boundaries of the copper grains in the corrosion process. Since the top and bottom parts of the corroded CF-2 copper foil maintain a uniform corrosion pattern, this indicates that the orientation of the copper grains in the CF-2 copper foil always maintains the initial growth state during the electrodeposition process.

The cross-section morphology of CF-3 copper foil after corrosion shows that the surface of the corroded copper foil is smooth and flat. In contrast, the rough surface is corroded with fine particles corroded in the cross-section and relatively loose grains (Fig. 3c). The morphology of the corroded smooth surface and the bumpy surface is very different. This indicates that the growth direction of the grains changed during the deposition of CF-3 copper foil. The grain surface energy of the grains near the surface is higher, and the atoms are unstable. While the grain surface energy of the grains near the smooth surface is lower, which can remain stable and is not easy to corrode.

The cross-section morphology of CF-4 copper foil after corrosion shows that the morphology of the rough surface is similar to that of the smooth surface after corrosion. Only part of the grains have been corrupted. The overall morphology of the soft and flat area on the cross-section is close to that of the smooth area of the CF-3 samples, which suggests that the direction of the growth of the grains on the cross-section of the copper foil samples also maintains the direction of the early stage of the deposition of the copper grains (Figs. 3c,d).

The corrosion resistance of copper foils is closely related to the morphology and size of the deposited grains. Combined with the rough surface morphology of the copper foils, the grains of CF-2 and CF-4 copper foils are refined and compact, and the corrosion resistance of copper foils is relatively high; the grains of CF-1 copper foils are coarse, with irregular prismatic grain morphology, and the inter-granular porosity is apparent (Fig. 3), which is not conducive to the enhancement of corrosion resistance of copper foils; the grains of CF-3 copper foils are coarse, with loose inter-grain bonding, and the rough surface in the microstructure is not smooth, which is not conducive to the enhancement of corrosion resistance of copper foils. CF-3 copper foil has coarse grains, loose bonding between grains, large fluctuations in the roughness of the microstructure, and roughness that is not smooth, which is not conducive to the improvement of the corrosion resistance of the copper foil.

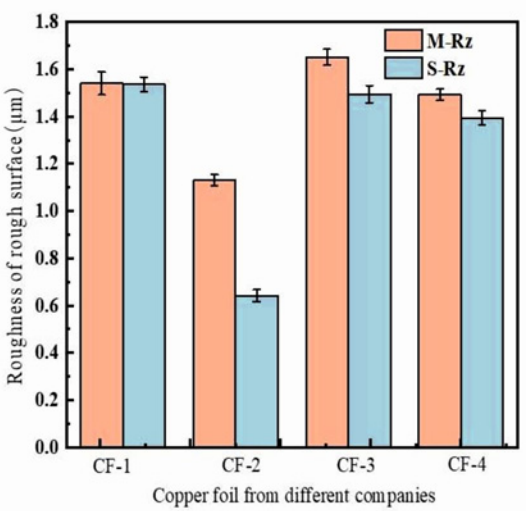

Fig. 4. S/M roughness of 6 μm copper foil from different companies.

3.2. Roughness

The side of the copper foil close to the cathode rollers in the production process is called the S-surface, and the other is called the M-surface. The roughness of the smooth (S-surface) and rough (M-surface) surfaces of the copper foils of the companies were tested. The roughness of CF-1 copper foil is close to that of the smooth surface, which is about 1.50 μm; CF-2 copper foil has the lowest roughness among the four plants, with a smooth surface roughness of 0.65 μm, which is much lower than that of its rough surface, which is 1.13 μm. The surface roughness of the copper foils designated CF-3 and CF-4, was observed to be higher. Furthermore, the roughness of the rough surface was found to exceed that of the smooth surface for both foils (Fig. 4).

In the process of electrodeposition of copper foil, the surface near the side of the cathode roller is called the smooth surface. The morphology of the smooth surface of the copper foil replicates the cathode roller morphology. Generally speaking, because the cathode roller is in a high temperature and robust acid environment for a long time, its surface is rough, making it difficult to peel the copper foil. Therefore, after a while, polishing and polishing are carried out to keep the surface roughness of the cathode roller at a low level, and the smooth surface morphology of the copper foil as the morphology of the cathode roller after replication; the roughness will be very low. Based on the cathode roller with low roughness, copper foil is

Table 1. Grain size, residual stress, and texture coefficient of 6 μm copper foil from different companies

Sample number	Producer	Grain size (nm)	σ (10^6 N m^2)	Texture coefficient T_c (%)		
				(111)	(200)	(220)
Y1	CF-1	28	–30.04	52.52	20.85	15.02
Y2	CF-2	23	–18.05	62.46	22.49	8.37
Y3	CF-3	26	–29.69	20.88	19.94	49.60
Y4	CF-4	21	–27.15	41.62	34.08	11.40

electrodeposited on it, which can not only maintain the low roughness of the copper foil smooth surface but also reduce the roughness of the rough surface accordingly. The roughness of copper foil from each manufacturer also corresponds to its grain size. The smaller the grain size, the lower the roughness of the rough and smooth surfaces of the copper foil. The larger the grain size of the copper foil, the higher the roughness of its smooth and rough surfaces (see Table 1). Therefore, the roughness of the cathode roller is kept at a low level during production. Combined with the appropriate production process, copper foil with a small grain size and low roughness can be obtained.

3.3. Texture

Copper is a typical face-centered cubic metal. As its close-packed surface, the (111) crystal plane has the lowest energy, followed by the (200) crystal plane, and finally, the (220) crystal plane has the highest power. In the process of the copper foil section being corrupted, the lower the crystal surface energy is, the more stable it is, and the less likely it is to be corrupted. That is to say, the higher the proportion of (111) crystal surface of copper foil, the less likely it is to be corrupted, followed by (200) crystal surface, and the higher the proportion of (220) crystal surface, the worse the corrosion resistance of copper foil. The surface state of the cathode roll undergoes alteration during the electrodeposition process, which in turn affects the current distribution and the strength and uniformity of the electric field. This, in turn, determines the growth and nucleation processes of copper, as well as the crystalline orientation of the copper foil.

The grain orientation of the copper foils produced by different enterprises varies greatly, and in general, the copper foils produced by each factory have three textures, namely, (111), (200), and (220). Among them, CF-1 copper foil is preferentially orientated to the (111) grain surface, and the diffraction peak intensity of the (220) grain surface is higher than that of the (200) grain surface; CF-2 copper foil is also preferentially orientated to the (111) grain surface, but the diffraction peak intensity of the (200) grain surface is higher than that of the (220) grain surface. The diffraction peak intensity of the grain surface of CF-3

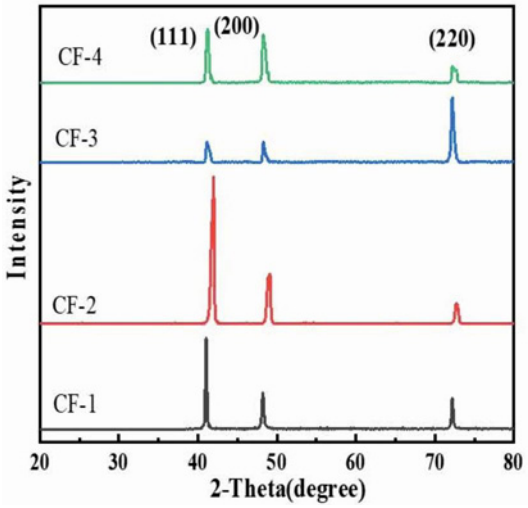

Fig. 5. XRD of 6 μm copper foil matte surface of different companies.

copper foil differs significantly from that of the first two enterprises. This copper foil is mainly oriented in the (220) crystal plane, and the diffraction peak intensities of the (111) and (200) crystal planes are comparable, and both are at a lower level; the last type of CF-4 copper foil is preferentially oriented in the (111) crystal plane, with the diffraction peak intensity of the (200) crystal plane being the second highest, and the diffraction peak intensity of the (220) crystal plane being lower (Fig. 5). To analyze the differences in the preferred paths of the textures of the copper foils of the different enterprises more precisely, the texture coefficients of each crystalline plane were calculated using Scherrer's formula. CF-1, CF-2, and CF-4 Cu foils have relatively high proportions of (111) crystalline planes, with texture coefficients of 52.5, 62.5, and 41.6 %, respectively. (200) crystalline planes have the highest proportion of (200) crystalline planes of CF-4 Cu foils, with texture coefficients of 34.1 %, and (220) crystalline planes of CF-3 Cu foils have the highest proportion of (220) crystalline planes, with 49.6 % (Fig. 6).

From the corrosion patterns of the copper foils' cross sections, the CF-2 and CF-4 copper foils were in good condition after corrosion. The CF-2 copper

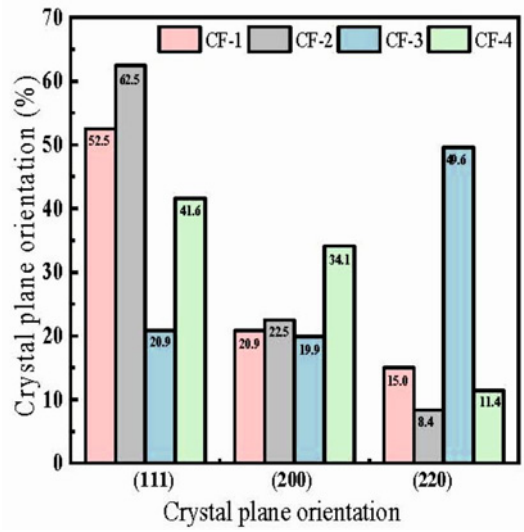

Fig. 6. Proportion of 6 μm copper foil matte surface of different companies.

foils did not have large holes due to the loosening and detachment of the grains after corrosion. The CF-4 copper foils had corrosion particles in only the shallow area of the surface after corrosion, and they did not rust to the deeper layers (Fig. 3). The diffraction peaks of the copper foils had the highest intensities at the grain surface of (111), followed by the (200) surface. The diffraction peak intensities of the copper foils were relatively poor at the cross-section of CF-1 and CF-3 copper foils after corrosion. The diffraction peak intensities at the (200) surface were the highest, and the diffraction peak intensities were the highest at the (200) surface of the copper foil. CF-3 Cu foils have relatively poor cross-sections after corrosion. CF-3 Cu foil has the highest percentage of (220) crystal planes. Although CF-1 Cu foil has a relatively high proportion of (111) crystalline facets, the proportion of (200) crystalline facets is lower than that of CF-2 and CF-4, and the proportion of (220) crystalline facets is too high.

3.4. The relationship between grain size, texture, and residual stress

From the results of the grain size test, it can be seen that the grain size of the copper foils is CF-4 < CF-2 < CF-3 < CF-1, while the comparative results of the residual stresses of the copper foils are CF-2 < CF-4 < CF-3 < CF-1 (see Table 1). Meanwhile, from the results of the test of the residual stresses, it can be seen that the residual stresses are present in all four manufacturers and that the copper foils show compressive stresses in the planar surfaces. It can be seen that the CF-2 producer's copper foil has the lowest residual stress, and the grain size of this producer's copper foil is also tiny, about 23 nm. At the same time, the copper foil has the highest proportion of the (111) crystal plane, the lowest proportion of the (220) crystal plane, and the texture coefficient of the (200) crystal plane is much more significant than that of the (220) crystal plane. The value of the residual stress of the copper foil of CF-4 is lower than that of CF-2. The value of the residual stress of CF-4 is lower than that of CF-2. The value of the grain size of CF-4 is the smallest. The minimum grain size value of CF-4 is 21 nm, and the grain size of CF-4 is the smallest. It has the smallest grain size, and the foil has a firm (111) texture. Similar to CF-2, the texture coefficient of the (200) grain face of the copper foil is much larger than that of the (220) grain face, followed by CF-3 copper foil. The residual stress of this sample is higher than that of CF-4 and CF-2, and the grain size is larger than that of CF-2 and CF-4. The data show that this Cu foil has the lowest (111) facet orientation and a firm (220) texture, with the most significant percentage of facets; lastly, the CF-1 Cu foil has the highest residual stress, and the grain size of its Cu foil is also the largest. Although the (111) texture of the Cu foil is preferentially oriented higher, the proportion of (200) and (220) crystalline facets is similar.

From the above data analysis results, we conclude that the grain size and crystal orientation of copper foil affect the residual stress of copper foil. If you want copper foil with less residual stress during electrodeposition, the first is grain size regulation, which should be controlled at a low level. The second is the regulation of the proportion of crystal planes. The proportion of (111) crystal planes of copper foil should be the highest, and the proportion of (220) crystal planes should be the lowest so that the proportion of (220) crystal planes is much smaller than that of (200) crystal planes. Satisfying the above conditions can significantly reduce the residual stress of copper foil.

3.5. Mechanical properties

Tensile tests were carried out on different manufacturers' copper foils, and the elongation and tensile strength data at room temperature were obtained. The tensile strengths of CF-3 and CF-1 copper foils at room temperature are at a high level of 508.73 and 478.47 MPa, respectively. Still, the elongation at room temperature is low, with CF-1 having the lowest elongation of 2.95 %. In comparison, the elongations of CF-2 and CF-4 are as high as 7.45 and 7.39 %, but their tensile strengths are deficient. The lowest elongation at room temperature is 2.95 % for CF-1 copper foil, while CF-2 and CF-4 copper foils have elongation as high as 7.45 and 7.39 % at room temperature, but their tensile strengths are very low (Fig. 7).

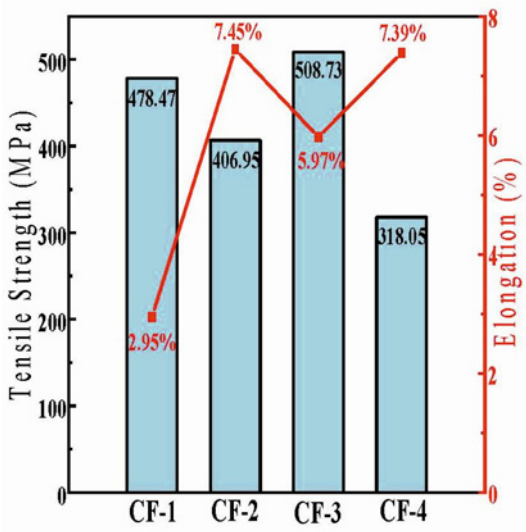

Fig. 7. Room temperature elongation and tensile strength of different enterprises.

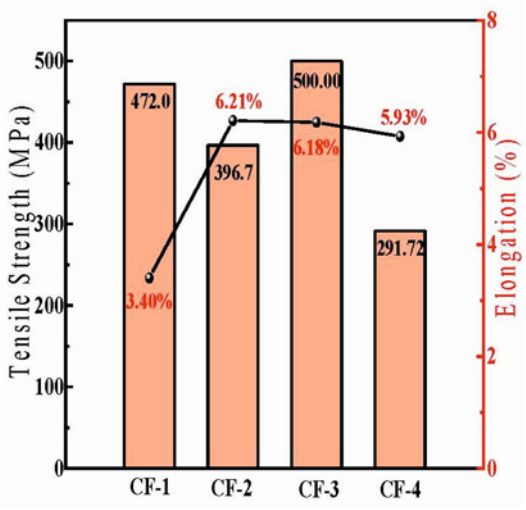

Fig. 8. High temperature (180 ℃) elongation and tensile strength of different enterprises.

The mechanical properties of copper foil are affected by its internal structure; first, the microstructure of CF-2 and CF-4 copper foils is more dense and uniform, and the bonding force between grains is more substantial, so they have better mechanical properties. Compared with CF-1, the grains of copper foils are coarse, and the edges and corners of grain morphology are too many, which is not conducive to the close bonding between grains. The microstructure of copper foils is loose, so it has poor comprehensive mechanical properties. The microstructure density of CF-3 copper foils is between the two, so the mechanical properties are also in the middle level. Secondly, from the perspective of grain size, the grain size of CF-1 and CF-3 copper foils is more prominent, and the grain size of CF-2 and CF-4 copper foils is smaller. The grain size determines the number of grain boundaries inside the copper foil. The smaller the grain size, the more grains inside the unit volume copper foil. In the process of tensile deformation, the same amount of deformation will be dispersed into more copper grains so that uniform deformation will occur so that the stress concentration will not be made, thereby reducing the possibility of local cracking. Therefore, the smaller the copper grain, the higher the elongation of the copper foil. Thirdly, from the perspective of grain boundary strengthening, the grain size of CF-3 copper foil is smaller than that of CF-1, and its room temperature elongation and tensile strength are also higher than those of CF-1 copper foil. The grain size of copper foil is fine, indicating that the number of grains in a unit volume of copper foil is large. Therefore, copper foil has more grain boundaries, and the grain boundary strengthening effect is better. Therefore, copper foil has high strength, and many grain boundaries can also prevent crack propagation in copper foil, increasing the room temperature elongation of copper foil. Finally, from the perspective of texture, CF-2 and CF-4 have a (111) preferred orientation, while the proportion of the (220) crystal plane is deficient. In contrast, CF-3 copper foil has a strong (220) preferred orientation, and CF-1 copper foil has a relatively high proportion of (220) crystal plane. Therefore, it is speculated that increasing the proportion of the (111) crystal plane is beneficial to improving the elongation of copper foil, and increasing the proportion of the (220) crystal plane is beneficial to improving the tensile strength of copper foil.

After testing the mechanical properties of the copper foils at room temperature, high-temperature tensile tests were also carried out. It can be seen that the mechanical properties of the copper foils from all manufacturers changed to varying degrees after being left in a closed environment at a high temperature of 180 ℃ for 1 min. The tensile strength and elongation of the CF-2 and CF-4 copper foils decreased significantly, but the elongation of the CF-1 and CF-3 copper foils increased significantly, with little change in tensile strength (Fig. 8).

In summary, the copper foils of CF-2 and CF-4 can maintain high elongation at room temperature and high temperature. Although the elongation is slightly reduced after high-temperature treatment, it is still at a high level. The mechanical properties of CF-3 copper foil at room and high temperatures did not change much, and the elongation at high temperatures only increased slightly. CF-3 copper foil was stable in both environments. Although the elongation of CF-1 copper foil under high-temperature conditions has been improved, it is still low, but the tensile strength still maintains this level.

4. Conclusions

This chapter mainly analyses the 6 μm lithium battery copper foil from different companies. The morphology of the rough surface, smooth surface, and cross-section of lithium copper foil is characterized by SEM. XRD compares and analyzes the texture of the copper foil. The performance of copper foil is obtained by roughness tester and tensile tester. The relationship between the copper foil's structure, morphology, and performance is obtained. The conclusions are as follows:

1. The titanium cathode roller affects the smooth surface morphology of fragile copper foil. In contrast, the rough surface morphology is closely related to the rough surface morphology and production process. The microstructure of the four typical copper foils is either refined grains or coarse columnar crystals. Therefore, to obtain fine-grained copper foil, it is necessary to use the cathode roller with low roughness as far as possible based on determining the process parameters.

2. The etching process affects the cross-sectional morphology of copper foil, and there are apparent differences in the corrosion resistance of the four typical copper foils: CF-2 > CF-4 > CF-1 = CF-3. Combined with the crystal orientation of copper foil, the corrosion resistance of CF-2 and CF-4 copper foils with (111) crystal plane is higher. In contrast, the corrosion resistance of CF-1 and CF-3 copper foils with (220) and (200) crystal planes is significantly reduced.

3. The residual stress of copper foil is affected by grain size and crystal orientation. If low residual stress copper foil is obtained, the grain size should first be controlled at a low level. Secondly, the (111) crystal plane of copper foil is the highest, the proportion of the (220) crystal plane is lower, and the proportion of the (220) crystal plane is much smaller than that of the (200) crystal plane, which can also significantly reduce the residual stress of copper foil.

4. The grain size and texture of copper foil are closely related to its mechanical properties. Firstly, with the decrease of grain size in copper foil, the tensile strength and elongation of copper foil gradually increase. Secondly, the increase in the proportion of the (111) crystal plane is beneficial to the growth of elongation, and the rise in the proportion of the (220) crystal plane is advantageous to the increase of tensile strength.

Acknowledgements

This work is supported by Shaanxi's critical research and development project, Province [Grant No. 2021SF--469], the National Natural Science Foundation of China [Grant No. 52175184], and Service Local Special Program of Education Department of Shaanxi Province (23JC051).

References

[1] J. Zhang, D. Zuo, X. Pei, C. Mu, K. Chen, Q. Chen, G. Hou, Y. Tang, Effects of electrolytic copper foil roughness on lithium-ion battery performance, Metals 12 (2022) 2110–2120. https://doi.org/10.3390/met12122110

[2] G. Li, H. Liu, H. Yang, X. Chen, K. Ji, D. Yang, S. Zhang, X. Ma, Tuning product distributions of CO_2 electroreduction over copper foil through cathodic corrosion, Chemical Engineering Science 263 (2022) 118142–118162. https://doi.org/10.1016/j.ces.2022.118142

[3] K. R. Gustavsen, E. A. Johannessen, K. Wang, Sodium persulfate pre-treatment of copper foils enabling homogenous growth of $Cu(OH)_2$ nanoneedle films for electrochemical CO_2 reduction, Chemistry Open 11 (2022) e202200133. https://doi.org/10.1002/open.202200133

[4] S. Zhang, H. Chen, Y. Qian, Y. Zhao, L. Suo, B. Zhang, W. Li, Effect of dealloying temperature on microstructure and tensile properties of self-supporting nanoporous copper foil fabricated in situ, Journal of Porous Materials 30 (2023) 267–276. https://doi.org/10.1007/s10934-022-01318-x

[5] K. Ding, F. Shi, Z. Zhang, B. Li, M. Di, M. Yan, L. Xu, X. Wang, H. Wang, Promoting effect of cobblestone-shaped CuI nanoparticles immobilized on the copper foil surface on the electrochemical performance of the conventional graphite electrode, International Journal of Electrochemical Science 17 (2022) 220965–220991. https://doi.org/10.20964/2022.09.61

[6] D. S. Yo, K. S. Wook, H. A. Jin, Fluorine-doped carbon quantum dot interfacial layer on stockade-like etched copper foil for boosting Li-ion storage, Chemical Engineering Journal 413 (2021) 127563–127598. https://doi.org/10.1016/j.cej.2020.127563

[7] M. A. Johar, A. Waseem, M. A. Hassan, I. V. Bagal, A. Abdullah, J. S. Ha, S. W. Ryu, Highly durable piezoelectric nanogenerator by hetero epitaxy of GaN nanowires on Cu foil for enhanced output using ambient actuation sources, Advanced Energy Materials 10 (2020) 2002608-2002618. https://doi.org/10.1002/aenm.202002608

[8] Z. Jingwei, Z. Kexin, M. Xiaoguang, Z. Jianlin, Study on the formability of copper foils during multi-step micro deep drawing, Journal of Materials Research and Technology 28 (2024) 2187–2198.

[9] Q. Li, X. Sun, W. Zhao, X. Hou, Y. Zhang, F. Zhao, X. Li, X. Mei, Processing of large-scale microporous group on copper foil current collectors for lithium batteries using femtosecond laser, Advanced Engineering Materials 22 (2020) 2000710. https://doi.org/10.1002/adem.202000710

[10] F. Zeng, C. Xue, H. Ma, C. T. Lin, J. Yu, N. Jiang, High thermal conductivity and anisotropy values of aligned graphite flakes/copper foil composites, Materials 13 (2020) 46–58. https://doi.org/10.3390/ma13010046

[11] Y. Wang, B. Zou, G. Yin, Wear mechanisms of Ti(C7N3)-based cermet micro-drill and machining quality during ultra-high speed micro-drilling multilayered PCB consisting of copper foil and glass fiber reinforced plastics, Ceramics International 45 (2019)

24578–24593.
https://doi.org/10.1016/j.ceramint.2019.08.187

[12] M. Georgiadou, R. Alkire, Anisotropic chemical etching of copper foil: I. electrochemical studies in acidic $CuCl_2$ solutions, Journal of The Electrochemical Society 140 (1993) 1340–1340.
https://doi.org/10.1149/1.2220981

[13] M. Wang, X. Zhang, L. L. Cheng, Q. Zhang, Bending fatigue damage behavior of annealed polycrystalline Cu foil, Materials Science Forum 971 (2019) 53–58.
https://doi.org/10.4028/www.scientific.net/MSF.971.53

[14] T.-D. Nguyen-Phan, C. Wang, C. M. Marin, Y. Zhou, E. Stavitski, E. J. Popczun, Y. Yu, W. Xu, B. H. Howard, M. Y. Stuckman, l. Waluyo, P. R. Ohodnicki, jr., D. R. Kauffman, Understanding three-dimensionally interconnected porous oxide-derived copper electrocatalyst for selective carbon dioxide reduction, Journal of Materials Chemistry A 7 (2019) 27576–27584. https://doi.org/10.1039/c9ta10135g

[15] J. Yu, W. Jing, E. Liu, S. Du, H. Cai, Sulfonated graphene oxide modified polysulfone-polyamide forward osmosis membrane and its application in fluorine-containing wastewater treatment, Materials Chemistry and Physics 313 (2024) 128757.
https://doi.org/10.1016/j.matchemphys.2023.128757